



RESEARCH ARTICLE

Silicon PV module fitting equations based on experimental measurements

Ahmad H. Sabry¹ | Wan Z. W. Hasan² | Yasameen H. Sabri³ |
Mohd Zainal Abidin Ab-Kadir^{1,4}

¹Institute of Power Engineering (IPE), College of Engineering, Universiti Tenaga Nasional (UNITEN), Kajang, Malaysia

²Department of Electrical and Electronics, Faculty of Engineering, University Putra Malaysia (UPM), Serdang, Malaysia

³Ministry of Electricity, Baghdad, Iraq

⁴Centre for Electromagnetic and Lightning Protection Research (CELP), University Putra Malaysia, Serdang, Malaysia

Correspondence

Ahmad H. Sabry, Institute of Power Engineering (IPE), College of Engineering, Universiti Tenaga Nasional (UNITEN), Kajang, Malaysia.
Email: ahs4771384@gmail.com

and
Wan Z. W. Hasan, Department of Electrical and Electronics, Faculty of Engineering, University Putra Malaysia (UPM), Serdang, Malaysia.
Email: wanzuha@upm.edu.my

Funding information

University Putra Malaysia, Malaysia, Grant/Award Number: Vot 9515302; University Tenaga Nasional (UNITEN)

Abstract

Solar photovoltaic (PV) characteristic curves (P-V and I-V) offer the information required to configure the PV system to operate as near to its optimal performance as possible. Measurement-based modeling can provide an accurate description for this purpose. This work analyzes the PV module performance and develops a mathematical formula under particular weather conditions to accurately express these curves based on a custom neural network (CNN). The study initially presents several standard mathematical model equations, such as polynomial, exponential, and Gaussian models to fit the PV module measurements. The model selection is subjected to the minimum value of an evaluation parameter. To simplify the solution of the symbolic equations for the CNN network, two neurons in the hidden layer with nonlinear activation function and linear for the output layer were selected. The results show the effectiveness of the proposed CNN model equations over other standard fitting models according to the root mean squared error (RMSE) evaluation. This method promises further improved results with multi-input parameter modeling.

KEYWORDS

curve fitting, custom neural network, I-V curve, mathematical modeling

1 | INTRODUCTION

As focusing on the current users of a solar photovoltaic (PV) energy, there is an unclear description and power profile for users in all PV sectors. There is a general need for all those PV users to get a better knowledge about their PV systems so as to gain the best efficient energy as compared with cost. In contrast, PV power is highly related to the weather conditions such

as; temperature and sun irradiance, which complicates the measurement optimizations, therefore, a modeling for such systems is an essential need.¹ A PV cell has a nonlinear current-voltage (I-V) characteristic that can be modeled using a current source, one or more diodes, and resistors. Single-diode and double-diode models are widely used to simulate PV characteristics. The single-diode model emulates the PV characteristics fairly and accurately.² The manufacturer provides information for the

PV electrical characteristics by specifying certain points on its I-V characteristics called remarkable points. The relationship between the voltage and current of a PV cell or module is summarized by the main electrical characteristics produced on typical solar cell P-V and I-V curves. The irradiance, which represents the intensity of the solar insolation incident on the module, controls the current (I), while the temperature rise reduces the module voltage (V).

A solar module produces direct current (DC), and the product of current and voltage provides the power (P). Therefore, we can create P-V curves representing the power versus the voltage for a given PV module. Since the relationship between the I-V and P-V characteristics is nonlinear for a PV system, analytical methods have been considered as a simple solution to model the behavior of a PV module.³ Mathematical modeling of a PV is described by the nonlinear relationship in the current-voltage (I-V) curve.⁴ Many researchers have proposed several models to describe the behavior of a PV cell and to improve the modeling and parameters estimation, such as those using the Lambert W function and numerically using the Newton-Raphson method.^{5,6} An artificial neural network (ANN) together with the Lambert W function were employed to determine the I-V and P-V curves of silicon and plastic solar cells and modules.⁷ Neural network adopts the principle of the human brain as a learning method to implement the functioning conditions between input/output, whether the system is a linear or nonlinear with a property of minimal computing processes.⁸ A comparative study in⁹ concludes that ANN-based models dominate and achieve better results than others such as; one-diode, multiple linear regression, polynomial regression, and analytical models. The main advantages of ANN-based approaches are that it does not require more complicated calculations or parameters, unlike other models. Under various weather conditions, the accuracy of PV power prediction has been improved by using the response characteristics of the PV array, and consequently, by measurements driven model power prediction methods.¹⁰ Efforts in¹¹ present seasonal meteorological features with historical data corresponding to different seasons by using optimized multi-layer back propagation neural network. The produced power profile of a Silicon-crystalline PV module has been estimated with reasonable accuracy in.^{9,12-15} The objective of the model estimation was to improve the prediction performance and evaluation using differences based on measures of accuracy to determine the root mean squared error (RMSE) or mean square error (MSE).¹⁶ A PV module is generally rated under standard test conditions (STC) with the solar irradiance (G) of 1000 W/m^2 , cell temperature (T) of 25°C , and AM 1.5 solar spectrum by the manufacturers. The parameters required for the input of the PV modules rely on the meteorological conditions of the area. The climatic conditions are unpredictable due to the random nature of their occurrence.

The above brief review concluded that the modeling of PV cell or array that is based on artificial intelligence approaches such as; ANN, Neuro-Fuzzy, etc., was applied in different conditions. Although these techniques have verified that the ANN is the most useful than classical methods, especially in terms of accuracy and simplicity, they did not present mathematical equations describing the power output or even the P-V/I-V characteristics. From this context, it is not clear, if the current modelings are scalable for providing more information that can assist PV power engineers to identify the harvested energy. The challenge of accurate modeling for the nonlinearity I-V characteristics of a solar cell can be solved through their matching with the experimental measurements. Therefore, offering efficient technique is essential to determine the model parameters precisely.

The rest of the paper is organized as follows; Section 2, briefly presents the main objective of the proposed modeling and the work contributions. This section includes two subsections: (a) the PV module manufacturer specifications and the experimental measurements, (b) the training algorithm of the proposed mathematical modeling and the approach topology. Section 3 discusses the obtained results and contains the proposed modeling results and a comparative study, which includes a brief review and comparison for the performance of the proposed CNN models with other standard data-fitting models, such as polynomial regression, exponential, Gaussian regression, and single-diode models. Finally, Section 4 concludes the research findings.

2 | PROPOSED MODELING

The main objective of this article was to develop an accurate and simple custom neural network (CNN) to extract mathematical representations of the P-V/I-V relationships for a PV module. The work also presents a comparison between different models to assess the performance of the proposed models. The comparison analyses help to choose the appropriate PV module in the design considerations of stand-alone PV and grid-connected systems.

The key contributions of this work are:

- Synthesizing the ANN architecture for a new topology to provide formulas for P-V and I-V relationship via a solvable set of nonlinear equations, which is achieved by acquiring experimental measurements at, appropriate sampling rate, data normalization, minimizing the hidden-layer neurons that have nonlinear activation functions (sigmoid), and output the result through a single-neuron with a linear function (pure-line).
- Estimating P-V/I-V characteristics and formulating the measured data with mathematical equations.
- Presenting a developed approach to analyze and model the PV module and its behavior.

2.1 | Module database

The system has a PV module, PHOTOWATT Silicon-Polycrystalline,¹⁷ the specifications are given in Table 1, while the I-V curves are shown in Figure 1.

All the analyses are performed using MATLAB software package. The experimental data measurement of P-V/I-V was conducted for a silicon solar module (polycrystalline) at an irradiance of 370 W/m² and a temperature of 28°C.

2.2 | Development of CNN-based mathematical model

The proposed CNN block diagram employed to estimate the P-V and I-V of the PV module is depicted in Figure. 2. The CNN has three layers, an input layer, a single hidden layer, and output layer. The input layer represented by a vector (V) of load voltage measurements in the first and second cases, while it has seven inputs; $[G, T, V_{oc}, I_{sc}, I_{MP}, V_{MP}, V]^T$ in the third case. The output layer has only single output neuron which is the current (I) in the first case or the power (P) produced by the PV module in the second and third cases.

The objective here was to find the input-output relation based on the experimental measurements.^{18,19} Moreover, to find whether an equation can be helpful to predict the power generated based on the seven inputs that previously mentioned. This equation can be formulated as follows:

$$I = f_{est}(V) \quad \text{case 1} \quad (1)$$

$$P = f_{est}(V) \quad \text{case 2} \quad (2)$$

$$P = f_{est}(G, T, V_{oc}, I_{sc}, I_{MP}, V_{MP}, V) \quad \text{case 3} \quad (3)$$

where f_{est} denotes the estimation/approximation function. The input-output data are subjected to the normalization process in order to get the more efficient network in terms of complexity and execution time, the general normalized data can be obtained from the following expression:

TABLE 1 Specifications of the PV module from the datasheet PHOTOWATT PV panel (Silicon Polycrystalline)

Specifications		Value
Maximum power P_{MAX}	W	55
Open circuit voltage V_{oc}	V	21.7
Short circuit current I_{sc}	A	3.4
Voltage, max power V_{MP}	V	17.3
Current, max power I_{MP}	A	3.2
Maximum system voltage	V	600 _{VDC}
Temperature coefficient for voltage (β)	mV/°C	-79
Temperature coefficient for current (α)	mA/°C	+0.95

$$x_{norm} = \frac{(x - x_{min})}{(x_{max} - x_{min})} \quad (4)$$

where x_{norm} denotes the normalized values of data x , where $x_{min} \leq x \leq x_{max}$. The same training algorithm has been implemented over the three proposed cases which are described in Figure 3.

Input-output data set is used to train the network over the training stage. After implementation of each input vector, the algorithm calculates the network output (I in case 1 or P in cases 2 and 3), that is consequently compared with the required output to create the Mean Square Error (MSE), this with a performance function is used for training the proposed CNN. The updated error is substituted in the Levenberg-Marquardt learning (learnLM) as an optimization algorithm to update the network weights and biases. Then, after sufficient iterations, MSE between the CNN and the target outputs stabilizes to a minimum quantity.

The network architecture of ($1 \times k$ for cases 1 and 2, and $7 \times k$ for case 3) input matrix, two hidden neurons, and a single output neuron has been used to model the PV-module characteristics' curves, where k is the number of measurements. At each iteration, each input vector (1×1 case 1 and 2, while 7×1 for case 3) is multiplied by their associated weights and passes through a nonlinear activation function (sigmoidal function) at the hidden layer. Next, the outcomes of the hidden neurons are also multiplied by their associated weights and processed with a pure-line activation function this time to simplify the solution for obtaining the algebraic equations. To summarize the architecture understanding, one case network is presented which is shown in Figure 4.

In general, since the output is configured as a linear transfer function, the formula for all cases is given by Equation 5, while the formula for each hidden-layer neuron is given by Equation 6:

$$I_{est} \text{ or } P_{est} = n_1^2 = \sum_{j=1}^2 (a_j L W_{1,j} + b_2) \quad (5)$$

Since the nonlinear activation function has been selected for the hidden layer, which is given by Equation 6, the outputs of these neurons (a_j) are given by Equation 7 for cases 1 and 2, and Equation 8 for case 3, as follows:

$$a_j = f_1(n_j^1) = \text{logsig}(n_j^1) = \frac{1}{1 + e^{-n_j^1}} \quad (6)$$

$$a_j = \frac{1}{1 + e^{-(V * I W_{(j,1)} + b_1)}} \quad \text{case 1 and 2} \quad (7)$$

$$a_j = \frac{1}{1 + e^{-(V_{oc} * I W_{(j,1)} + I_{sc} * I W_{(j,2)} + V_{MP} * I W_{(j,3)} + I_{MP} * I W_{(j,4)} + V * I W_{(j,5)} + G * I W_{(j,6)} + T * I W_{(j,7)} + b_1)}} \quad (8)$$

where n_j^1 denotes the hidden-layer summation formula, the upper subscript refers to the first layer which is the hidden one, and $j = 1, 2$, the number of hidden neurons. IW is the

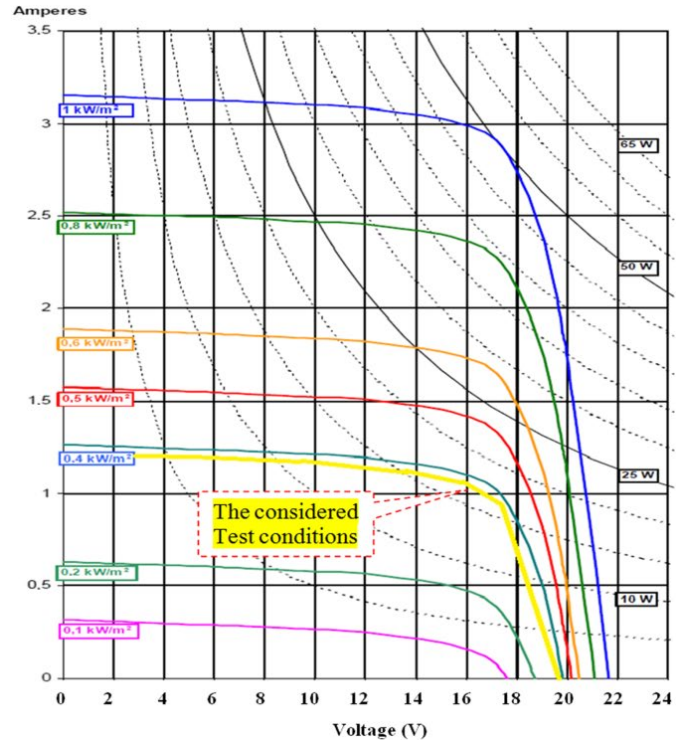
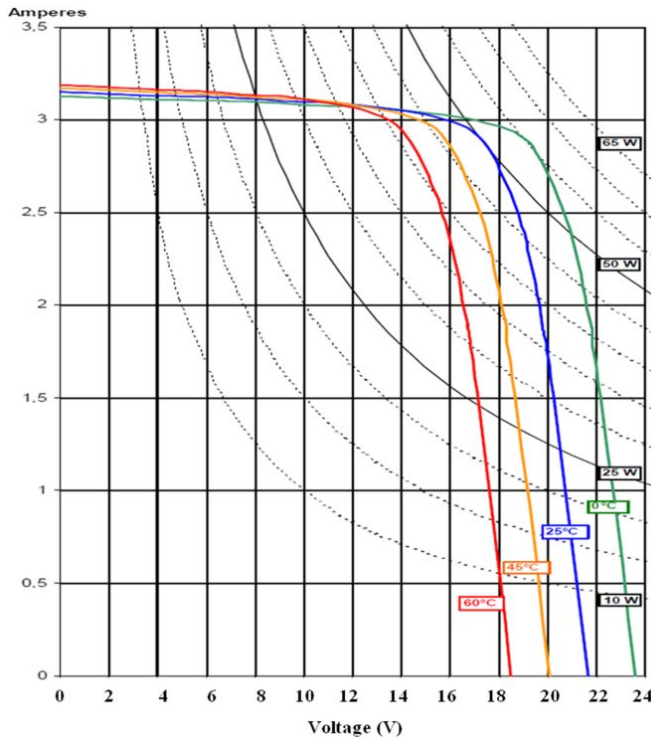


FIGURE 1 PHOTOWATT PV panel manufacturer I-V curves

input weight matrix, while b_1 and b_2 are the bias vector for the hidden and output layer neurons, respectively.

3 | RESULTS AND DISCUSSION

Experimental measurements have been implemented to find a set of data points that represent the current-voltage dataset (I_k, V_k) and the pairs of power-voltage data (P_k, V_k), where the index k represents the number of sampling data. In addition, to inspect the ability of the proposed CNN for modeling the profile of the PV-generated power precisely, the measurements along for about 8 days, cloudy and sunny, have also been conducted.

In order to present the conditions that affected the PV-module performance, multimeters are used to measure V_{oc} , I_{sc} , I_{MP} , and V_{MP} generated by the PV module. A variable resistor (0-120) Ω was considered as a load which implies the variation of the current and voltage. A temperature sensor to follow the temperature variation of the PV surface is also employed. Besides, a luxmeter (ISM 410) is used to follow the illumination. Figure 5 illustrates the PV schematic connections and experimental setup used to measure the characteristics $I = f(V)$.

3.1 | CNN model results

For case 1, which is similar to case 2, the correlation coefficient between the network and the target data is shown in

Figure 6 (A), while (B) shows the comparison between the proposed CNN model and the measured I-V profile. The relationship between the output and the target is evaluated by R -value. If there was an exact linear relationship between outputs and targets, R would be 1. Thus, if R is close to zero, this indicates that there is a nonlinear relationship between the outputs and the targets.²⁰ We have selected two related research articles that may benefit from the achievements of this work^{21,22} because they considered the solar PV array as the only power supply to feed electricity to a high-efficiency home system within a DC environment. This indicates that the training data have a great fitting result, and the proposed CNN fitting procedure for the current-voltage measurements is effective for this application.

In order to inspect the ability of the proposed CNN to model the pattern of the PV generated power precisely, about 8 days, cloudy and sunny, have been addressed, that is not been implemented during the training process of the proposed CNN. MSE has a great performance for the CNN model as shown in Figure 6. It is observed that the MSE over the training process approaches to 10^{-4} . This result indicates that the CNN weights are well updated and the approach could create output data of a reasonable accuracy for both sunny and cloudy days. According to Figure 7A, the best validation performance is 0.000133 at epoch 31, and the performance of the network was measured with R -square = 0.99972, as seen in Figure 7B. The results obtained a better goodness-of-fit than other relative models, which would be discussed later.

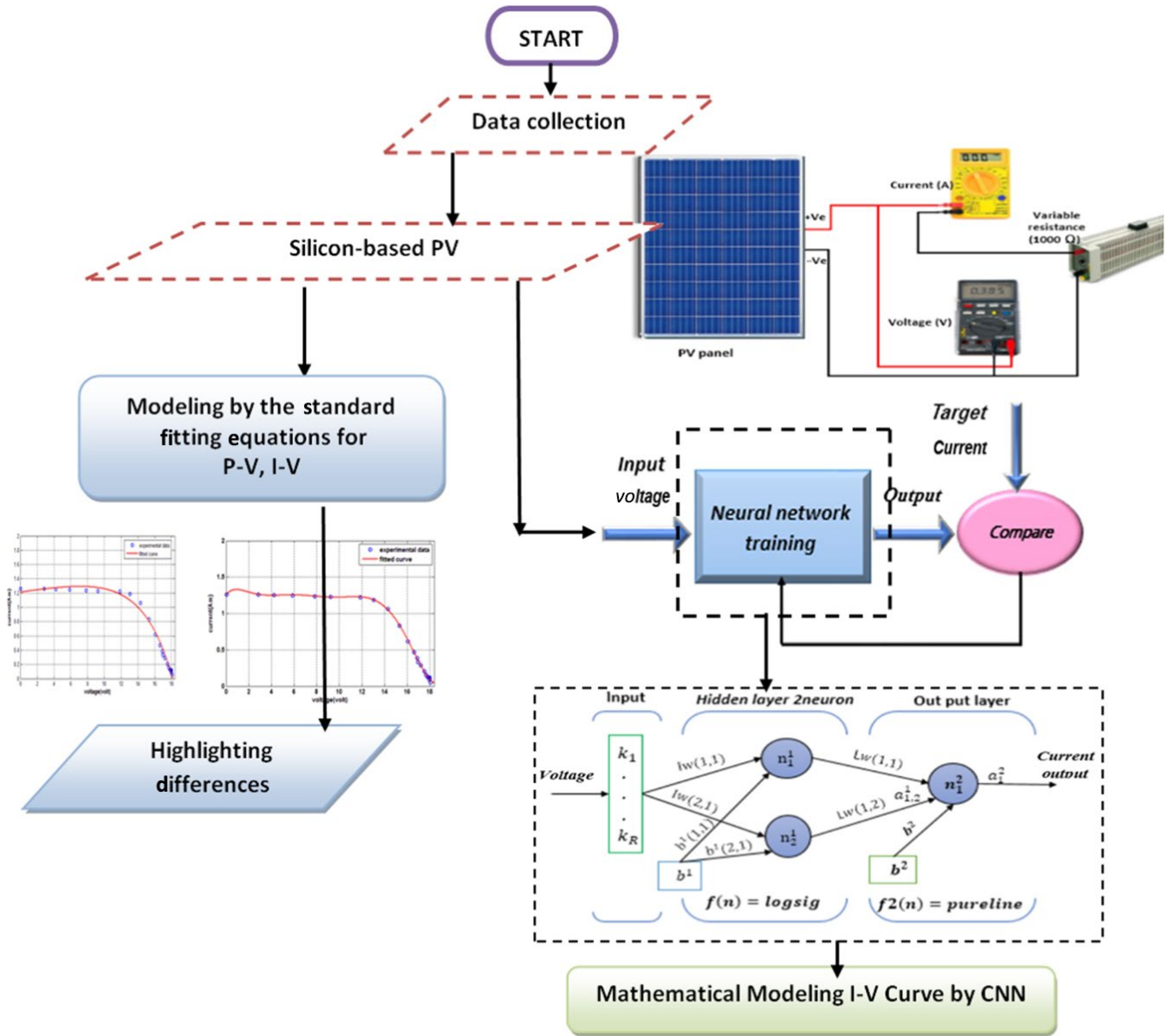


FIGURE 2 The concept of the proposed CNN

A superposition of curves is clear between the measurements and modeled/estimated patterns for the produced power of the PV module as shown in Figure 8. It is obvious that the measured values of the produced power are very close to the modeled/estimated one. A relatively matching of curves is clear between the measurements and modeled/estimated patterns for the produced power of the PV module.

By substituting the network weights, the equation of the output solar power (P) can be calculated as:

$$P = 1.25 - \frac{0.79682}{\left(1.008 * e^{(0.0377 I_{MP})} * e^{(0.0445 I_{sc})} * e^{(0.6377 V_{oc})} * e^{(0.4179 * V)} * e^{(0.496 * V_{MP})} + 1.0\right)} - \frac{1.42773}{\left(75574.82 * e^{(0.0871 I_{MP})} * e^{(0.1123 I_{sc})} * e^{(0.6377 V_{oc})} * e^{(-0.885 V)} * e^{(0.987 G)} * e^{(-0.456 T)} + 1.0\right)} \quad (9)$$

3.2 | Comparative analysis

In this section, a brief review and comparison of the performance for the proposed CNN models with other various models such as polynomial regression, exponential, Gaussian regression, and single-diode models are discussed.

3.2.1 | Modeling with fitting equations

Modeling and analysis using the I-V and P-V curve fitting method were performed in Specific LabVIEW and MATLAB software applications.²³ Data-driven modeling techniques can create models that are used when there is no sufficient information about a system. Therefore, these techniques can provide a model with a reasonable accuracy by choosing a

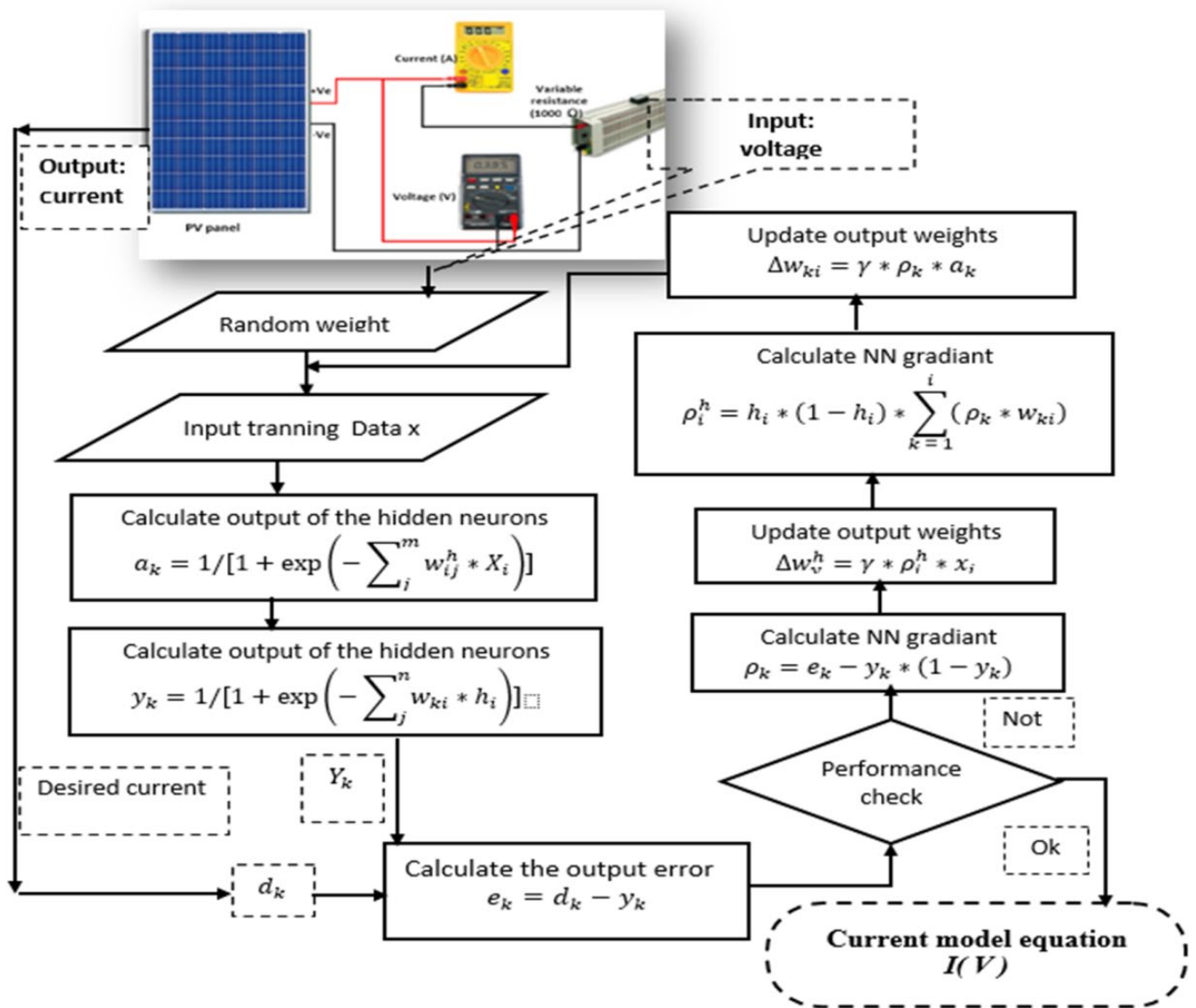


FIGURE 3 Training algorithm diagram of the proposed CNN modeling

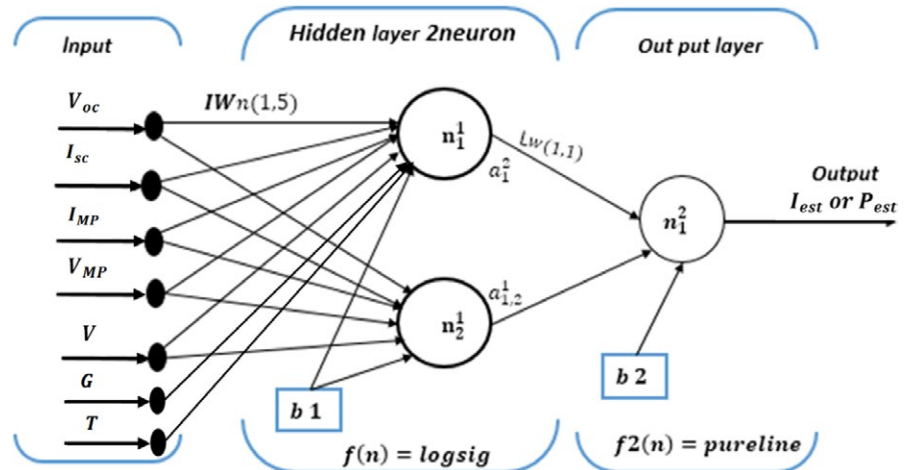


FIGURE 4 Proposed CNN architecture

suitable modeling technique. Curve fitting is a tool used to explore the relationships between data sets. This work investigates several models, such as polynomial, exponential, and

Gaussian, to obtain the equivalent function approximation for each of the current (I) as a function of a voltage (V), $I = f(V)$, and the module power (P) as a function of its voltage $P = f(V)$.

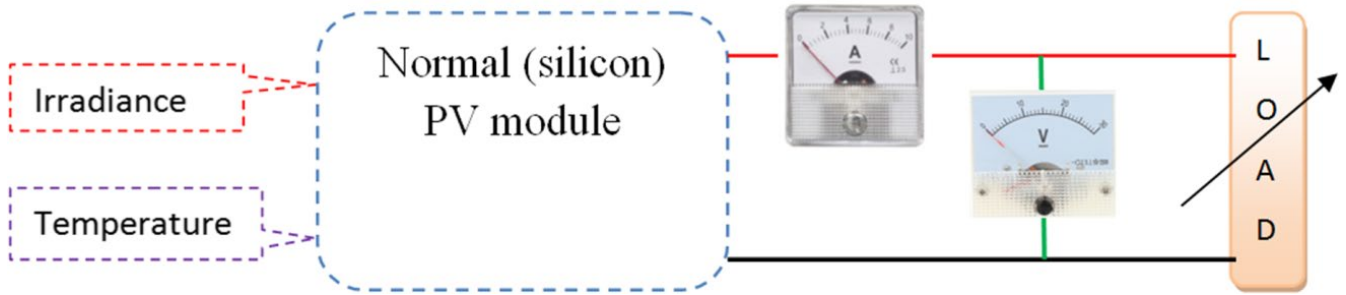


FIGURE 5 Photovoltaic schematic connection and experimental setup

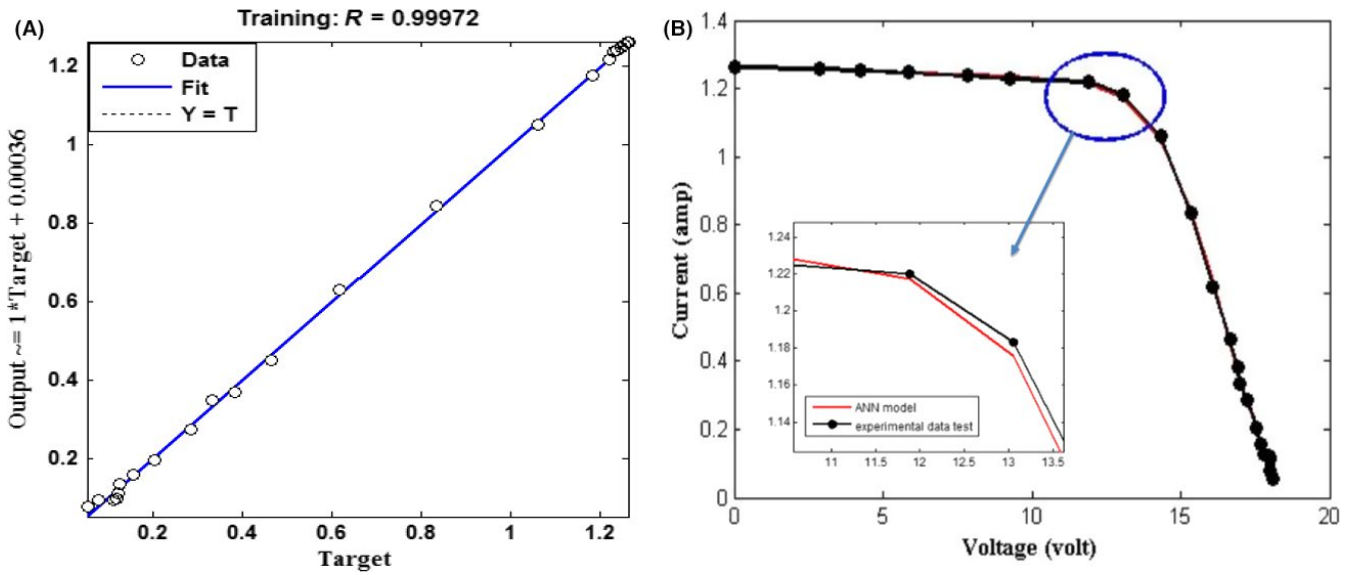


FIGURE 6 A, The correlation coefficient between the network and the target data. B, Comparison between the proposed CNN model and the measured I-V profile

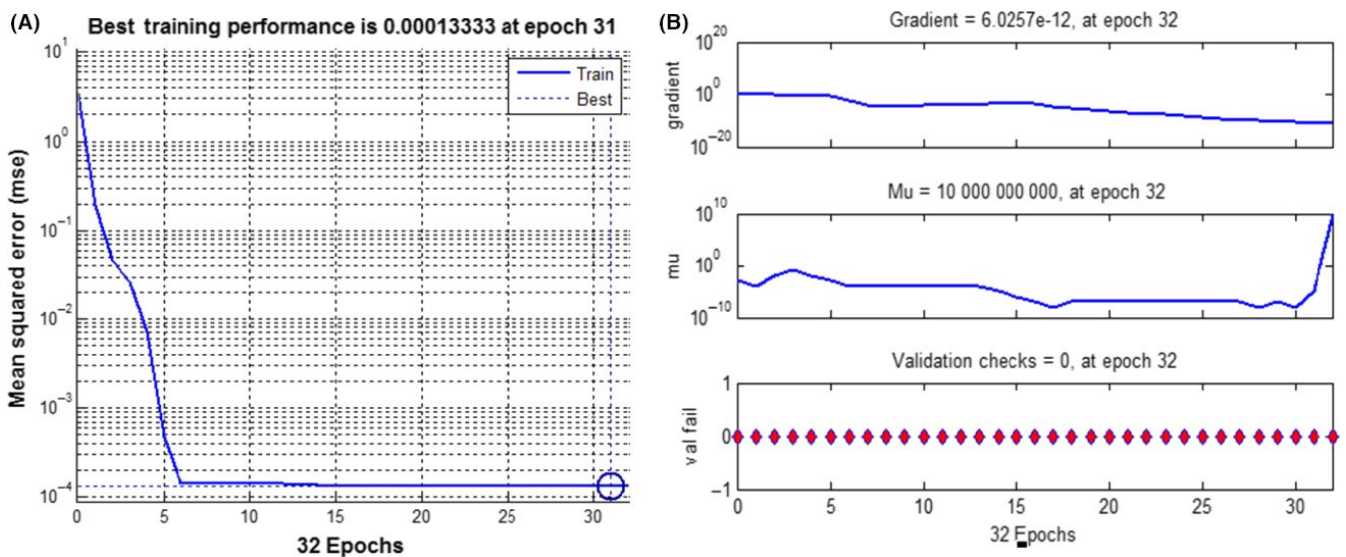


FIGURE 7 A, The training performance for the CNN with two neurons. B, Training state for the CNN model

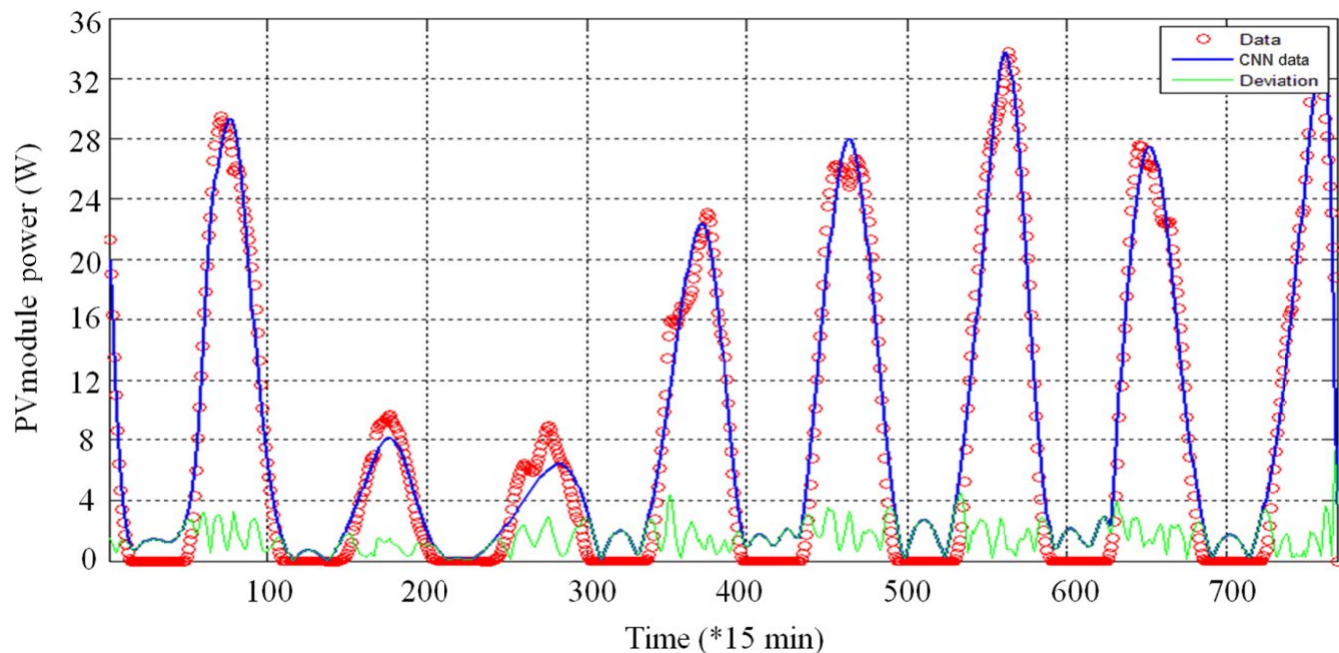


FIGURE 8 Comparison between measured data and modeled/estimated (CNN) of the produced power profiles of the used PV module for about 8 days

Table 2 provides a list of the common fitting equations used in MATLAB's built-in functions.²⁴ Some of the listed equations may fit one data set but not the others, and the fitting accuracy depends on the selection of the equation order. There is no dominant fitting approach for the types of observations in this paper, even for physical applications. Therefore, it is essential to consider the performance of several statistical methods to fit particular I-V and P-V curves to select the best one for a given measured data set.

Where $\beta_1, \beta_2 \dots \beta_9$ denote the coefficients of the polynomial model, while $a, \epsilon, \rho, b, d, \gamma$ denote the coefficients of the exponential and Gaussian models. In this research, all the experimental measurements of the data sets are marked with red circles in each graph.

As a case 1, the (I_k, V_k) experimental data points have been compared with the polynomial regression of degree 2-8, as shown in Figure 9A, the exponential of degree 1-2, and Gaussian of degree 2 models as depicted in Figure 9B.

As a case 2, the modeling of the (P_k, V_k) experimental data points with the polynomials of degrees 2-8 is shown in Figure 10A, exponential of degrees 1 and 2, and Gaussian of degree 2 models, as shown in Figure 10B.

To determine whether those models have a good approximation for the measured data, the goodness-of-fit statistics, such as the root mean square error (RMSE), the sum of squares due to error (SSE), a total sum of squares (SST), and R-square were used. The above all are calculated as follows:

$$\begin{aligned}
 SSE &= \sum_k^n (f(x_k) - y_k)^2 \\
 MSE &= SSE/v \\
 MSE &= \frac{1}{v} \sum_k^n (f(x_k) - y_k)^2 \\
 RMSE &= \sqrt{(MSE)}, \\
 SST &= \sum_k^n (f(x_k) - \frac{1}{n} \sum_k^n f(x_k))^2 \\
 R\text{-square} &= 1 - (SSE/SST)
 \end{aligned} \tag{10}$$

The index v indicates the number of independent portions of information involving the n data points required to calculate the sum of squares, $f(x_k)$ is a function of the input measured data (x_k, y_k) of the fitted model, k represents the number of sampling data measurements, and Y_k is an element of the data set (x_k, y_k) . Similar to the SSE, values of the MSE closer to zero indicate a better fit. The best fitting is obtained for the (I_k, V_k) , case 1 data and the power-voltage (P_k, V_k) case 2 data were based on the values of the RMSE. Therefore, for the experimental (I_k, V_k) data, case 1, the best fit curves are represented by the polynomial 8th degree regression and the exponential 2nd degree regression, as shown in Figure 11A and B, respectively.

For the (P_k, V_k) experimental data, case 2, the polynomial model of degree 6 and the Gaussian model of degree 2 were satisfied the minimum RMSE and the comparison can be shown in Figure 12.

The above evaluation for the addressed models or fitting equations shows that their application is effective and feasible to provide P-V and I-V mathematical models. Therefore,

TABLE 2 List of models for general mathematical equations

Model names	Degree	Equations
Polynomial model	1	$Y = \beta_1 x + \beta_2$
	2	$Y = \beta_1 x^2 + \beta_2 x + \beta_3$
	3	$Y = \beta_1 x^3 + \beta_2 x^2 + \beta_3 x + \beta_4$
	8	$Y = \beta_1 x^8 + \beta_2 x^7 + \dots + \beta_9$
Exponential model	1	$Y = \alpha.e^{(b.x)}$
	2	$Y = \alpha.e^{(b.x)} + \gamma.e^{(d.x)}$
Gaussian model	1	$Y = \alpha_1 e^{-(\frac{x-\mu_1}{\epsilon_1})^2}$
	2	$Y = \alpha_1 e^{-(\frac{x-\mu_1}{\epsilon_1})^2} + \alpha_2 e^{-(\frac{x-\mu_2}{\epsilon_2})^2}$
	3	$Y = \alpha_1 e^{-(\frac{x-\mu_1}{\epsilon_1})^2} + \dots + \alpha_8 e^{-(\frac{x-\mu_8}{\epsilon_8})^2}$

the satisfied fitting equations are the polynomial regression, exponential, and Gaussian regression models. Therefore, we can briefly describe the models that satisfy reasonable fitting evaluation as follows:

- Case 1, I-V curve, $I = f(V)$: 8th degree of Polynomial model Equation 11, or the 2nd order Exponential model, Equation 12, as follows:

$$I(V) = \beta_1 V^8 + \beta_2 V^7 + \dots + \beta_8 V + \beta_9 V^0 \quad (11)$$

$$I(V) = \alpha.e^{(b*V)} + \gamma.e^{(d*V)} \quad (12)$$

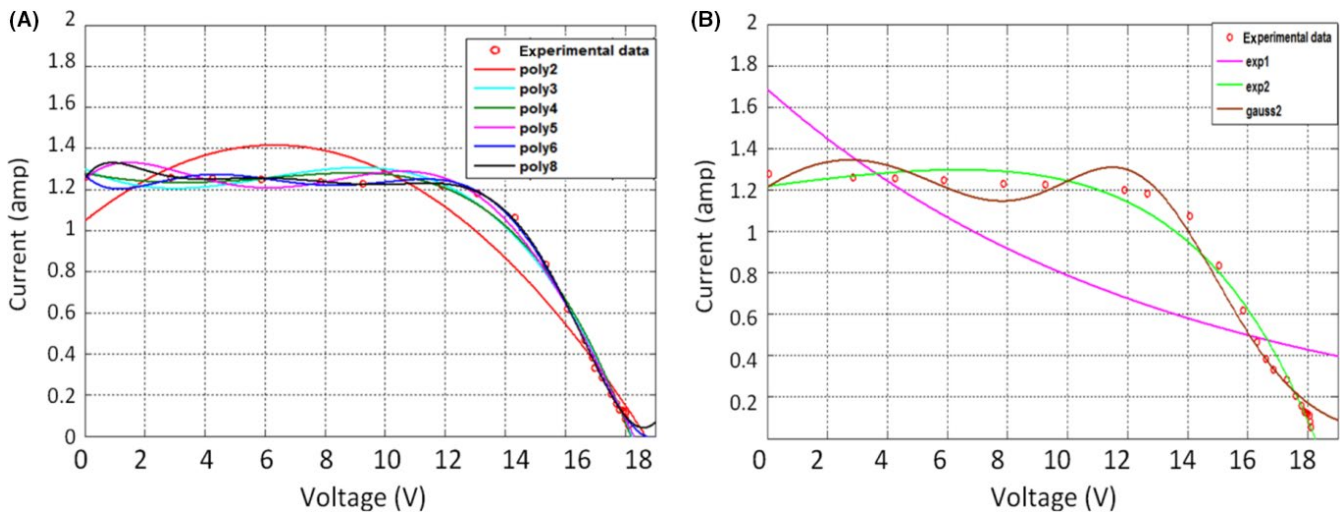


FIGURE 9 The modeling of the (I_k, V_k) experimental data points with (A) polynomials of degrees 2-8; (B) exponentials of degrees 1 and 2 and Gaussian of degree 2

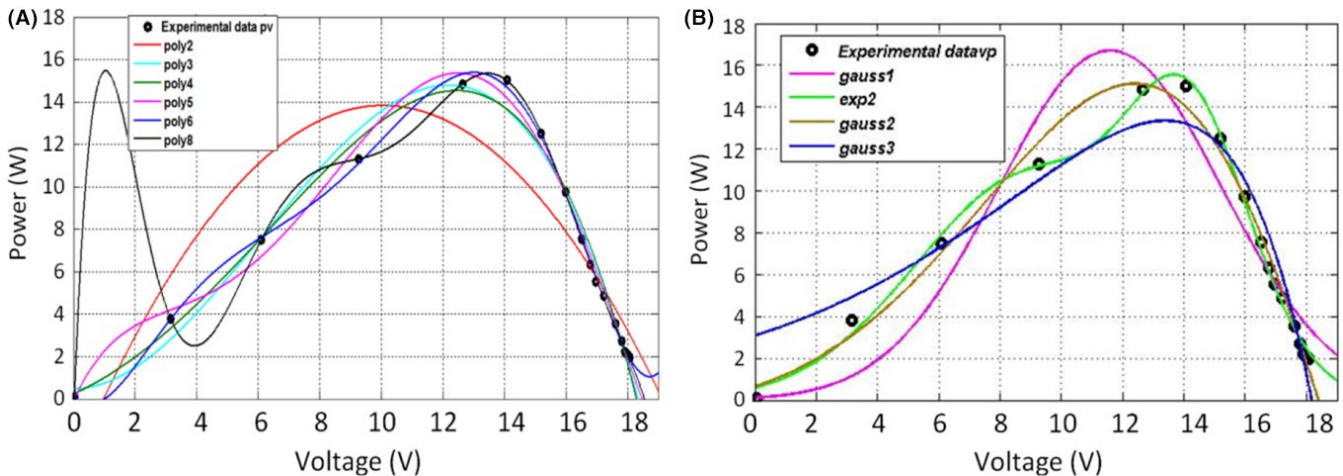


FIGURE 10 The modeling of the (P_k, V_k) data test with the (A) polynomials of degrees 2-8; (B) exponential of degree 2 and Gaussians of degrees 1, 2, and 3

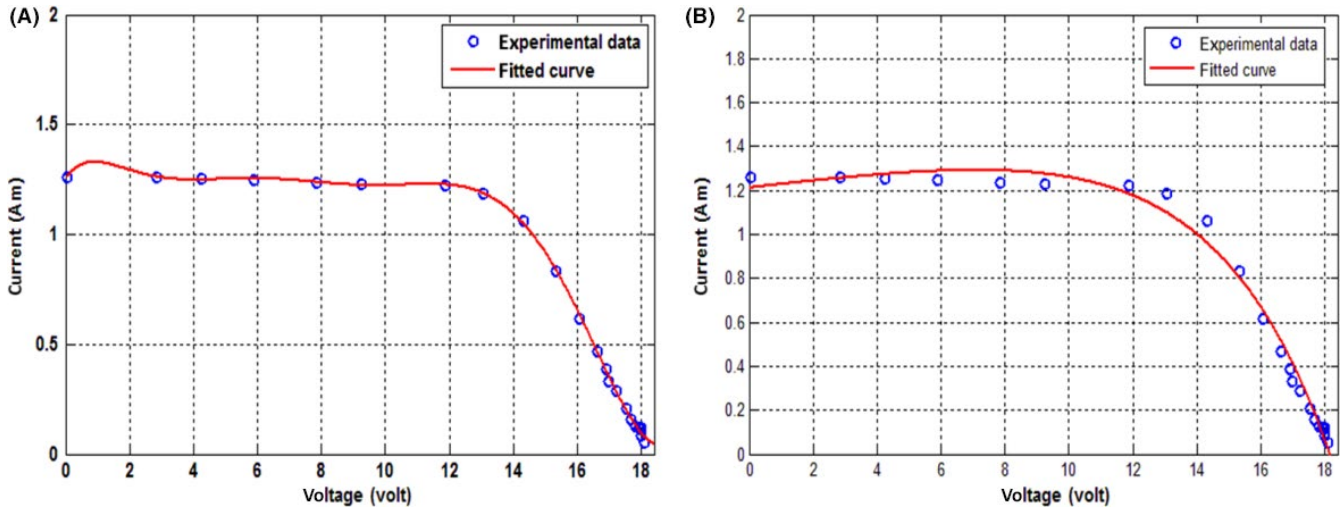


FIGURE 11 The best fitting result for the measurement (I_k, V_k) data with (A) an 8th degree polynomial model with RMSE = 0.0151 and (B) 2nd degree exponential model with RMSE = 0.0533

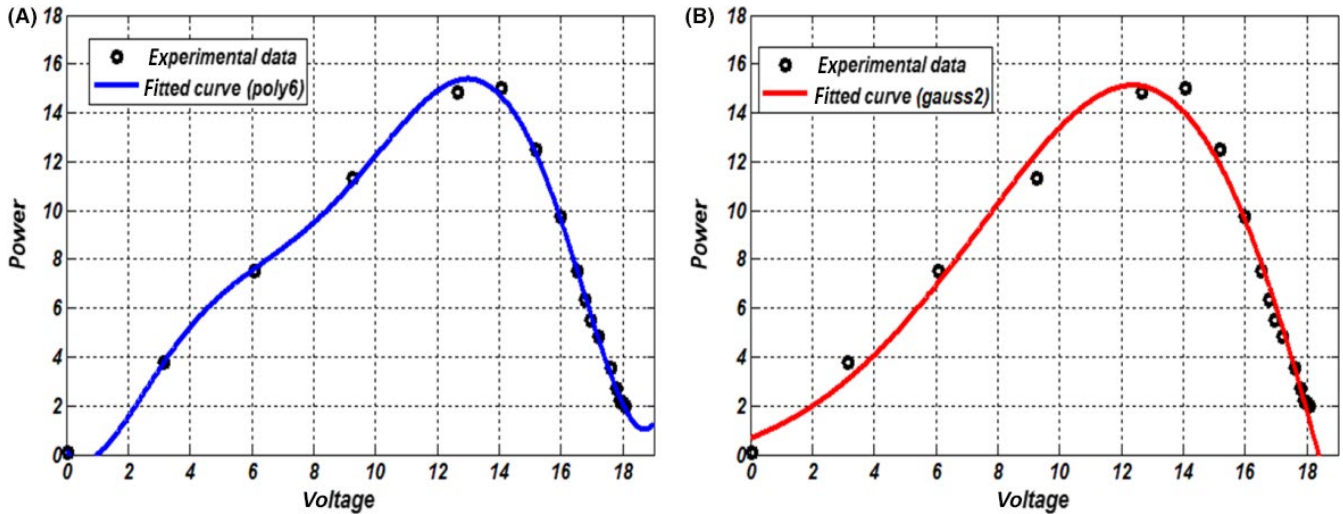


FIGURE 12 Modeling results of the experimental data power curve (P_k-V_k) fit with (A) a polynomial model of degree 6 with RMSE = 0.2338; (B) a Gaussian model of degree 2 with RMSE = 0.4040

- Case 2, P-V curve, $P = f(V)$: 6th degree of Polynomial model Equation 13, or the 2nd order of Gaussian model, Equation 14, as follows:

$$P(V) = \beta_0 V^6 + \beta_1 V^5 + \dots + \beta_5 V^1 + \beta_6 V^0 \quad (13)$$

$$P(V) = \alpha_1 \cdot e^{-((V-\rho_1)/\epsilon_1)^2} + \alpha_2 \cdot e^{-((V+\rho_2)/\epsilon_2)^2} \quad (14)$$

where $\beta, \alpha, \gamma, \epsilon, \rho, b, d$ denote the fitting coefficients. The fitting evaluation parameters for the approximate of I-V and P-V characteristic curves are listed in Table 3.

The fitted curves show some matches to the experimental data. The accurate fitting of (V, I, P) is highly influenced by the higher degree for each case.

3.2.2 | Single-diode model

The modeling process assists in knowing the characteristics and physical components of the solar cell. An accurate performance prediction reflects the modeling but requires the design of a model with sufficiently balanced complexity and accuracy.²⁵ The most commonly used model is the traditional single-diode model in parallel with a light generated current source I_{PH} , a series resistor R_S , and a shunt

Figures		Modeling type	R^2	RMSE	SSE
Current-voltage	11(a)	Polynomial 8th	0.9994	0.0151	0.0032
	11(b)	Exponential 2nd	0.9903	0.0533	0.0541
Power-voltage	12(a)	Polynomial 6th	0.9984	0.2338	0.6011
	12(b)	Gaussian 2nd	0.9946	0.4040	1.9585

TABLE 3 The fitting evaluation parameters for both I-V and P-V

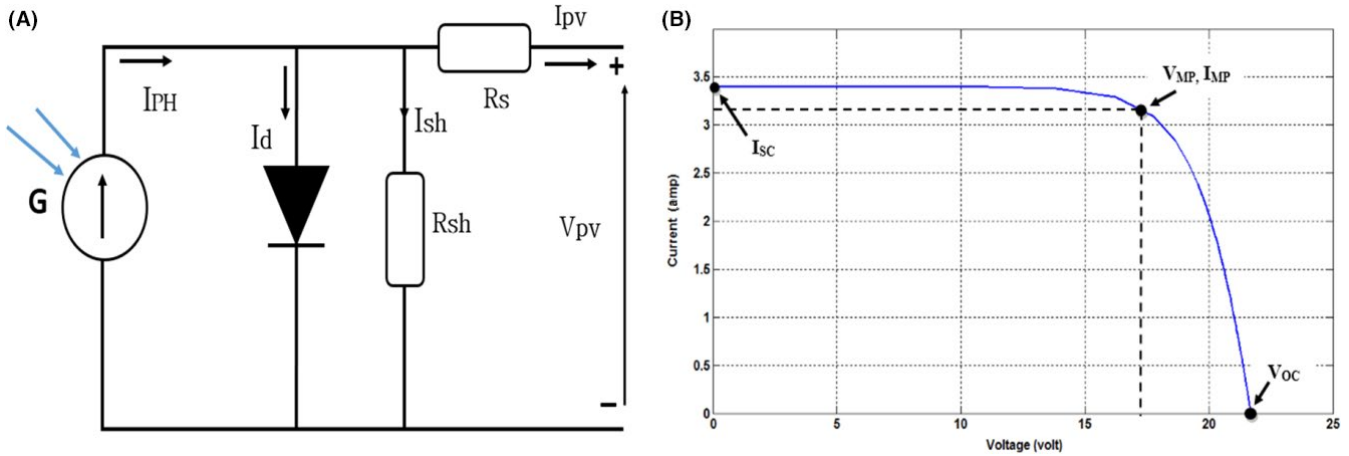


FIGURE 13 A, Equivalent circuit of the single-diode model. B, The I-V characteristic curve of a PV cell

resistor R_{Sh} , as shown in Figure 13A, also known as the five-parameters model.^{26,27} A general equivalent equation of a single-diode model of the current-voltage output characteristics can be expressed mathematically as in Equation 15:

$$I = I_{PH} - I_s \left[\exp \left(\frac{q(V + IR_s)}{KT_c A} \right) - 1 \right] - (V + IR_s) / R_{sh} \quad (15)$$

where I_{PH} is the photocurrent, I_s is the saturation current, $q = 1.6 \times 10^{-19} C$ is an electron charge, $K = 1.38 \times 10^{-23} J/K$ is Boltzmann's constant, T_c is the working temperature (Kelvin), A is an ideal factor, R_{Sh} is the shunt resistance, and R_s is the series resistance, while I_d and I_{Sh} denote the diode and shunt resistance currents. Thus, an equivalent circuit is used together with the equivalent equation to express a model for the current-voltage characteristic (I-V) curve of a PV cell or module. The most useful terms are the open circuit voltage V_{oc} , the short circuit current I_{sc} , and the current and voltage at the maximum power point (I_{MP} and V_{MP}), respectively, as shown Figure 13B.

The (I-V) characteristic curves of the measured data are verified through a MATLAB simulation. The simulation has been designed for the same solar module that we have tested experimentally according to the data listed in Table 1. The developed Simulink MATLAB design is shown in Figure 14.

The results of the simulation are obtained as a P-V and I-V curves, that are used as a reference to compare them with each of the experimental and the proposed model. To verify the measured and modeled I-V curves, a Simulink MATLAB program was used, and the results are shown in Figure 15.

After repeating the I-V measurements in three time-consecutive under the same weather conditions, it is noted that three nonidentical curves of I-V have created, as well as the simulation and the CNN-model curves. It is worth mentioning that the CNN model has used the last test data for training its network (measurements3). It is obvious that the maximum value of I_{sc} in the simulation is almost the same as in measurements1, which is the first testing attempt in terms of time. The I_{sc} provided by the manufacturer is 3.4 Amp under STC (see Table 1), but since our weather conditions were at $370 W/m^2$ and $28^\circ C$, then the measured $I_{sc} = 1.26$ Amp is an acceptable value, and the difference between the simulation and real measurements is about 0.002 Amp (see Table 4). It is also noted that the experimental measurements are not the same but are closer to the simulation results in measurements1 where the ambient temperature was $28^\circ C$ for the cells and the irradiance fixed at $370 W/m^2$, the difference in V_{oc} is below 0.7 V (20.1 V simulated and 19.43 V in measurements1).

After three consecutive testing attempts over time, the difference in measurements is significant, which in turn indicates that there is a power loss of about 1.7W (17.1W simulated

The proposed model was validated using the measured I-V characteristics, the results are compared and illustrated in Table 4. It is obvious that the CNN model is capable of accurately simulating the characteristics of the module with a good agreement between the two curves.

Figure 16 displays a comparison of the I-V curve by each of the experimental measurements, the eighth order polynomial fitting equation, and the proposed CNN model.

CNN-model results were also verified by comparing the experimental results with the manufacturer datasheet, which proves the effectiveness of the proposed modeling method.

4 | CONCLUSIONS

Modeling process assists in knowing the characteristics of physical components of the solar cell. The paper covered basically several models (Polynomial, Exponential, Gaussian, and single-diode Models), to approximate the experimental measurements of $I(V)$ and $P(V)$, and $P(G, T, V_{oc}, I_{sc}, I_m, V_m, V)$. The work compares those models with the CNN-based mathematical model. The results show various fitting accuracy and depend on different factors for each individual method. The addressed approaches of PV models can facilitate the design and characteristic analysis for different types of solar PV module/cell.

The proposed model (CNN) is a simple architecture which is developed to model and estimate the profile of the generated power of a 55 W polycrystalline PV module. The ability of the CNN to estimate the PV generation has been satisfied with reasonable accuracy. This work demonstrates that

the CNN models perform better than that by the polynomial, exponential, Gaussian, and the traditional single-diode models. CNN allows determination of electrical parameters for a PV module and the assessment of the power generated for any conditions at a constant temperature and solar irradiance.

The stepwise process for modeling the PV module helps to persuade more scholars into PV study and will give an idea of perceptive of I-V and P-V attribute of a PV panel. Except for it, such a representation would offer a systematic tool to envisage the behavior of future solar module under climate and physical parameter changes.

As a future work it is possible to design an equivalent circuit which can reflect the behavior of the solar cell/module, and even the PV array after the training is accomplished. This is done by using the analogue computer schemes, where each

TABLE 4 Comparison of the module output current among the experimental, CNN output, and simulation results

$V_{\text{experimental/input}}$	$I_{\text{experimental}}$	$I_{\text{CNN model}}$	$I_{\text{Simulation}}$
18.01	0.112	0.099	0.1125
17.93	0.123	0.122	0.123
17.7	0.157	0.1571	0.157
16.98	0.332	0.331	0.332
16.56	0.466	0.457	0.451
15.35	0.735	0.845	0.78
14.33	1.062	1.058	1.153
11.89	1.22	1.216	1.254
5.88	1.248	1.246	1.257
2.86	1.26	1.2606	1.258

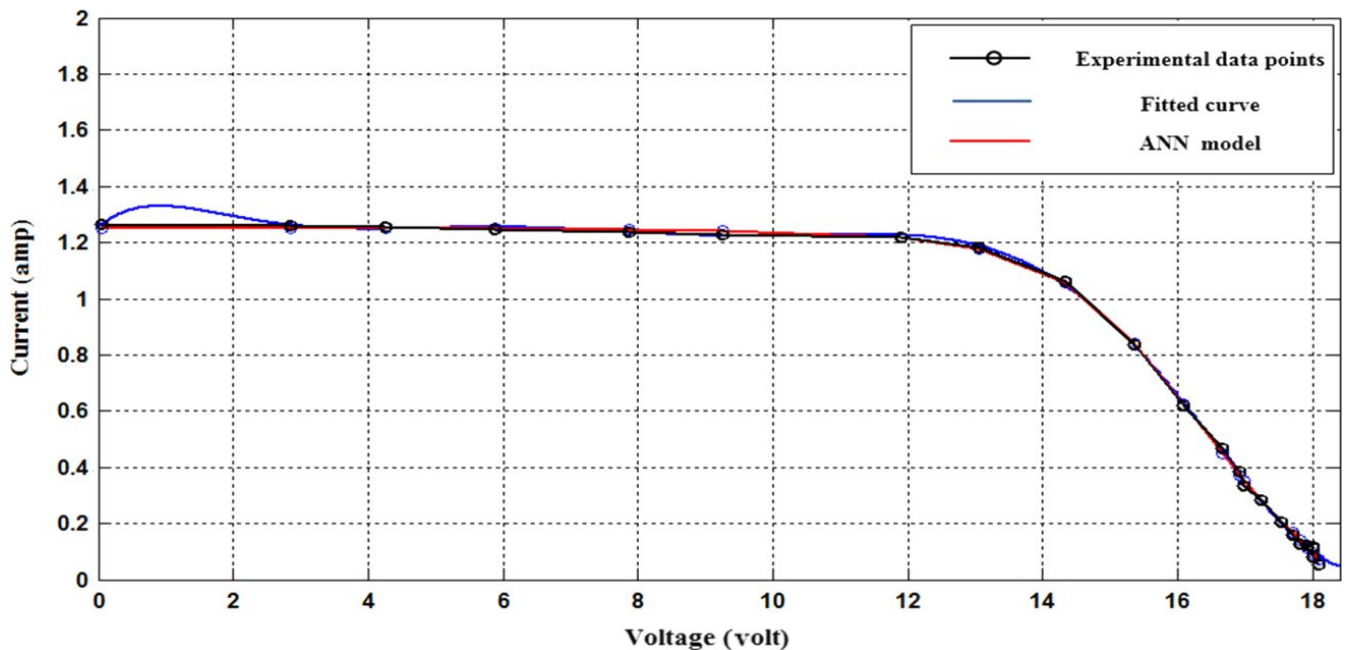


FIGURE 16 I-V Comparison by each of the experimental measurements, the eighth order polynomial fitting equation, and the proposed CNN model

neuron can be represented by op-amp summer circuit. The values of the resistors are equivalent to the network weights. For the neurons that have linear activation functions, the summer op-amp circuit can satisfy the linearity behavior. But, for neurons of nonlinear activation functions, another one or two op-amp circuit can be employed to present the nonlinearity action on the output of the summer amplifier. As consequently, a network of passive and active electronic components can achieve this modeling.

ACKNOWLEDGMENTS

This research was supported partly by the University Putra Malaysia, Malaysia (Grant: Vot 9515302) and by University Tenaga Nasional (UNITEN).

ORCID

Ahmad H. Sabry  <https://orcid.org/0000-0002-2736-5582>

REFERENCES

- Cubas J, Pindado S, de Manuel C. Explicit expressions for solar panel equivalent circuit parameters based on analytical formulation and the Lambert W-function. *Energies*. 2014;7:4098-4115.
- Rahim NA, Ping HW, Selvaraj J. Photovoltaic module modeling using Simulink/Matlab. *Procedia Environ Sci*. 2013;17:537-546.
- Villalva MG, Gazoli JR, Ruppert Filho E. Modeling and circuit-based simulation of photovoltaic arrays. In: *2009 Brazilian Power Electronics Conference, COBEP2009*, 2009:1244-1254.
- Zhang C, Zhang J, Hao Y, Lin Z, Zhu C. A simple and efficient solar cell parameter extraction method from a single current-voltage curve. *J Appl Phys*. 2011;110(6):1-7.
- Zainal NA, Yusoff AR. Modelling of photovoltaic module using matlab simulink. *IOP Conf Ser Mater Sci Eng*. 2016;114(1):012137.
- Abdulkadir M, Samosir AS, Yatim AHM. Modeling and simulation based approach of photovoltaic system in Simulink model. *ARPN J Eng Appl Sci*. 2012;7(5):616-623.
- Izadian A, Pourtaherian A, Motahari S. Basic model and governing equation of solar cells used in power and control applications. In *2012 IEEE Energy Convers. Congr. Expo. ECCE 2012*, no. September 2012, 2012:1483-1488.
- Bimenyimana S, Bimenyimana S, Norense G, Asemota O, Lingling L. Output power prediction of photovoltaic module using nonlinear autoregressive neural network. 2, no. August, 2017:32-40.
- Mellit A, Sağlam S, Kalogirou SA. Artificial neural network-based model for estimating the produced power of a photovoltaic module. *Renew. Energy*. 2013;60:71-78.
- Saberian A, Hizam H, Radzi MAM, Ab Kadir MZA, Mirzaei M. Modelling and prediction of photovoltaic power output using artificial neural networks. *Int J Photoenergy*. 2014, 2014.
- Hu Y, Lian W, Han Y, Dai S, Zhu H. A seasonal model using optimized multi-layer neural networks to forecast power output of pv plants. *Energies*. 2018;11:326.
- Xiao W, Nazario G, Wu H, Zhang H, Cheng F. A neural network based computational model to predict the output power of different types of photovoltaic cells. *PLoS ONE*. 2017;12:e0184561.
- Poudel P, Jang B. Solar power prediction using deep learning technique. *Adv. Sci. Technol. Lett*. 2017;146:148-151.
- Almonacid F, Rus C, Hontoria L, Fuentes M, Nofuentes G. Characterisation of Si-crystalline PV modules by artificial neural networks. *Renew. Energy*. 2009;34:941-949.
- Almonacid F, Rus C, Hontoria L, Muñoz FJ. Characterisation of PV CIS module by artificial neural networks. A comparative study with other methods. *Renew. Energy*. 2010;35:973-980.
- Fathabadi H. Novel neural-analytical method for determining silicon/plastic solar cells and modules characteristics. *Energy Convers Manag*. 2013;76:253-259.
- Sanyo, PHOTOWATT PW500 – 12V, 33, no. January, 2009.
- Chatterjee A, Keyhani A, Kapoor D. Identification of photovoltaic source models. *IEEE Trans Energy Convers*. 2011;26(3):883-889.
- Khatib T, Mohamed A, Sopian K, Mahmoud M. Assessment of artificial neural networks for hourly solar radiation prediction. *Int J Photoenergy*. 2012;2012:1-7.
- Jolson Singh K, Kho KLR, Jitu Singh S, Chandrika Devi Y, Singh NB, Sarkar S. Artificial neural network approach for more accurate solar cell electrical circuit model. *Int J Comput Sci Appl*. 2014;4(3):101-116.
- Sabry AH, Hasan WZW, Ab Kadir MZA, Radzi MAM, Shafie S. DC-based smart PV-powered home energy management system based on voltage matching and RF module. *PLoS One*. 2017;12:(9).
- Sabry AH, Hasana WZW, Kadir MZAA, Radzi MAM, Shafie S. Low cost wireless sensor monitoring system for photovoltaic (PV) array parameters. in *2017 IEEE 4th International Conference on Smart Instrumentation, Measurement and Application (ICSIMA)*, 2017, no. November, pp. 1-6.
- Chen Y, Wang X, Li D, Hong R, Shen H. Parameters extraction from commercial solar cells I-V characteristics and shunt analysis. *Appl Energy*. 2011;88(6):2239-2244.
- Sabry AH, Hasan WZW, Ab Kadir MZA, Radzi MAM, Shafie S. Field data-based mathematical modeling by Bode equations and vector fitting algorithm for renewable energy applications. *PLoS One*. 2018;13(1):e0191478.
- Shokrzadeh S, Jafari Jozani M, Bibeau E. Wind turbine power curve modeling using advanced parametric and nonparametric methods. *IEEE Trans Sustain Energy*. 2014;5(4):1262-1269.
- El Tayyan AA. An approach to extract the parameters of solar cells from their illuminated I – V curves using the Lambert W function. *Turkish J Phys*. 2015;39(1):1-15.
- Balogun EB, Huang X, Lin Y, Liao ZM, Adaramola MF. Regression estimation modelling techniques on static solar photovoltaic module. *Int. J. Emerg. Technol. Adv. Eng*. 2015;5:451-461.
- Spanoche SA, Stewart JD, Hawley SL, Opris IE. Model-based method for partially shaded PV module hot-spot suppression. *IEEE J. Photovoltaics*. 2013;3:785-790.

How to cite this article: Sabry AH, Hasan WZW, Sabri YH, Ab-Kadir MZA. Silicon PV module fitting equations based on experimental measurements. *Energy Sci Eng*. 2019;7:132–145. <https://doi.org/10.1002/ese3.264>